Journal Pre-proofs

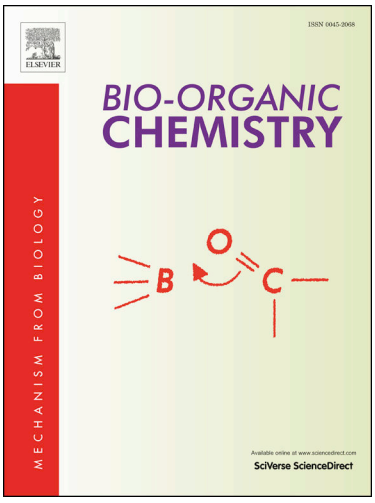

Novel Linezolid Analogues with Antiparasitic Activity against *Hymenolepis nana*

Eleazar Alcántar-Zavala, Esteban Hernández-Guevara, Adrián Ochoa-Terán, Julio Montes-Ávila, Edgar A. Estrada-Zavala, Alex J. Salazar-Medina, Efraín Alday, Alberto Cabrera, Gerardo Aguirre, Valentín Miranda-Soto, Carlos Velazquez, Sylvia P. Díaz-Camacho, José L. Medina-Franco

PII: S0045-2068(20)31657-6
DOI: https://doi.org/10.1016/j.bioorg.2020.104359
Reference: YBIOO 104359

To appear in: *Bioorganic Chemistry*

Received Date: 3 September 2020
Revised Date: 22 September 2020
Accepted Date: 5 October 2020

Please cite this article as: E. Alcántar-Zavala, E. Hernández-Guevara, A. Ochoa-Terán, J. Montes-Ávila, E.A. Estrada-Zavala, A.J. Salazar-Medina, E. Alday, A. Cabrera, G. Aguirre, V. Miranda-Soto, C. Velazquez, S.P. Díaz-Camacho, J.L. Medina-Franco, Novel Linezolid Analogues with Antiparasitic Activity against *Hymenolepis nana*, *Bioorganic Chemistry* (2020), doi: https://doi.org/10.1016/j.bioorg.2020.104359

Novel Linezolid Analogues with Antiparasitic Activity against *Hymenolepis nana*

Eleazar Alcántar-Zavala,[1] Esteban Hernández-Guevara,[2] Adrián Ochoa-Terán,[1]* Julio Montes-Ávila,[3]* Edgar A. Estrada-Zavala,[3] Alex J. Salazar-Medina,[4] Efraín Alday,[5] Alberto Cabrera,[1] Gerardo Aguirre,[1] Valentín Miranda-Soto,[1] Carlos Velazquez,[5] Sylvia P. Díaz-Camacho,[6] José L. Medina-Franco[7]

[1] Centro de Graduados e Investigación en Química, Tecnológico Nacional de México/IT de Tijuana. Tijuana, B.C., México.

[2] Facultad de Ciencias Químicas e Ingeniería, Universidad Autónoma de Baja California campus Tijuana. Tijuana, B. C. México.

[3] Facultad de Ciencias Químico Biológicas, Universidad Autónoma de Sinaloa. Culiacán, Sin. México.

[4] Cátedras Conacyt - Departamento de Investigación en Polímeros y Materiales, Universidad de Sonora. Hermosillo, Sonora, México.

[5] Departamento de Ciencias Químico-Biológicas, Universidad de Sonora. Hermosillo, Sonora, México.

[6] Environment and Health Research Unit, Autonomous University of Occident, Los Mochis, Sinaloa, México.

[7] Departamento de Farmacia, Facultad de Química, Universidad Nacional Autónoma de México. Ciudad de México, México.

*Correspondence author e-mail: ochoa@tectijuana.mx, jmontes@uas.edu.mx

Abstract

The stereoselective synthesis and anti- *Hymenolepis nana* activity of six Linezolid-type compounds, obtained by chemical modification of L-Alanine, are reported in this work. The synthetic strategy was to prepare diasteromeric *N*,*N*-dibenzylamino oxazolidinones **1** and **2**, and coupling with 4-(4-bromophenyl)morpholine (**3**) to obtain *N*,*N*-dibenzylamino

Linezolid analogues **4** and **5**. A hydrogenolysis reaction over **4** and **5** resulted in amino-free Linezolid analogues **6** and **7**, which were acetylated to reach diasteromeric Linezolid analogues **8** and **9**. The six Linezolid analogues **4-9** show *in vitro* antiparasitic activity against *Hymenolepis nana* cestode, but not against several bacterial strains. Interestingly, compounds **6**, **7** and **9** exhibit high potency, having shorter paralysis and death times after exposure (6 to 10 and 18 to 21 min, respectively), shorter than those found with antihelmintic compound Praziquantel (20 and 30 min) at 20 mg/mL. In addition, a cytocompatibility assay of **6-9** with human cells (ARPE-19 cells) demonstrate a non-cytotoxic effect at 0.4 mM. These results show the pharmacological potential of the newly reported Linezolid-type analogues as antiparasitic agents against *Hymenolepis nana*.

Keywords: Linezolid analogues; antiparasitic activity; stereoselective synthesis

1. Introduction

Intestinal parasitosis is a public health problem which affect 60 % of worldwide population.[1] Among a wide number of well-known parasite organisms, *Hymenolepis nana* (*H. nana*) and *Hymenolepis diminuta* cestodes are recognized as the principal hymenolepiasis infective agents. Hymenolepiasis is consider as a neglected disease affecting about 175 million of people around the world.[2] *H. nana* is a parasite capable to complete its biological cycle inside a single host. Although this infection is not fatal, it does have significant morbidity.[3] This is a cosmopolite disease, but a higher prevalence is present in countries with a tropical climate, affecting mainly school age children, elderly and immunocompromised adults. In addition, there is a higher prevalence in the lower income population countries, and it is associated to bad hygiene habits. Commonly, this is an asymptomatic illness, but its clinical manifestations are diarrhea, stomachache, headache, weight loss and poor nutrient absorption.[3-6] Praziquantel is the drug traditionally used to treat intestinal or tissue cestodial parasitosis. However, recent studies have revealed resistance of *H. nana* to praziquantel, as well as hepatotoxic, genotoxic and carcinogenic side effects.[6] Calcium ion (Ca^{2+}) channels are the only moiety identified as the molecular target of Praziquantel by indirect evidence, showing high affinity for

membrane receptors, affecting the cellular membrane permeability, promoting the fast Ca^{2+} absorption and inducing damages in the tegument of some parasites.[7,8]

Linezolid is the first commercially available antibiotic with a 1,3-oxazolidin-2-one structural base. It was first synthesized in 1990 by Pharmacia-Upjohn laboratories (now Pfizer) and approved by the FDA in 2000. This drug is used for treatment of nosocomial infections caused by multi-resistant Gram positive bacterial strains as methicillin-resistant *Staphylococcus aureus* (MRSA), penicillin-resistant *Staphylococcus epiderminis* (PRSE), penicillin-resistant *Spreptococcus pneumoniae* (PRSP), vancomycin-resistant *Enterococcus faecium* and *Enterococcus faecalis* (VREF).[9-13] In addition, the activity of Linezolid against *Mycobacterium tuberculosis* has been proved.[14] This drug inhibits the initiation and translation phases in the synthesis of bacterial proteins by intercalation between the 30S and 50S ribosomal subunits.[15,16] Linezolid structure consists in of oxazolidinone ring (A ring), a fluorophenyl ring (B ring), a morpholine ring (C ring) and an acetamide methyl substituent with a specific *S* configuration in C5 position of the A ring (Figure 1).[17]

Oxazole compounds have been described as bioactive molecules valuable for medicinal chemistry, showing a broad spectrum of biological activities, including antiparasitic properties.[18] However, there are few studies in the literature focused on the antiparasitic activity of Linezolid or analogues. These reports conclude in null activity, which justifies its exclusive use as an antibacterial agent.[19,20]

Previously, we reported the stereoselective synthesis and antibacterial activity of a series of *N*,*N*-dibenzylamino 1,3-oxazolidin-2-ones prepared by chemical modification of α-amino acids. The oxazolidinone derived from L-alanine **1** showed significant activity against Methicillin Resistant *Staphylococcus aureus* (MRSA) isolated strains.[21,22] In this work, by using diasteromeric oxazolidinones **1** and **2** as precursors, we report the synthesis of six new analogues having the characteristic structure of Linezolid (A, B and C rings) with some modifications such as a) the presence of a chiral center and a methyl group attached to the ring A substituent, b) variation in the configuration of the oxazolidinone chiral center (*S* or *R*) and c) different substituents in the amino group (benzyl, hydrogen or acetyl) (Figure 1). Remarkable results were found in antiparasitic activity assays, suggesting the anti- *H. nana* potential of these oxazolidinone compounds. To the best of

our knowledge, this is the first report of Linezolid-related compounds with antiparasitic activity.

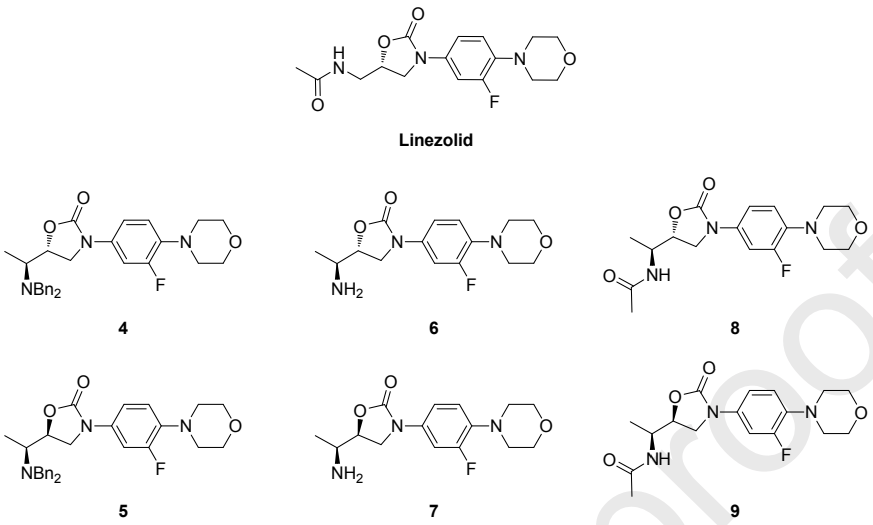

Figure 1. Linezolid and Linezolid-analogues structure.

2. Experimental

2.1 Chemical synthesis

***N-aryl coupling of oxazolidinones 1 and 2 with 4-(4-bromo-2- fluorophenyl)morpholine* (3).**

To a solution of the oxazolidinone (**1** or **2**)[21,22] (0.32 moles), CuI (0.01 mmol), K_2CO_3 (0.53 mmol), 4-(4-bromo-2-fluorphenyl)morpholine (**3**) in toluene (25 mL) was added dropwise the *N*,*N′*-dimethylmethanediamine (0.06 mmol). Then, the reaction mixture was stirred at 115°C for 72 h. Finally, water (25 mL) was added to finish the reaction and the organic phase was separated, filtered using zeolite and evaporated under vacuum. The product purification was carried out by flash chromatography on silica gel and a mobile phase of petroleum ether and ethyl acetate (1:1).[23,24]

***(R)*-5-((*S*)-1-(dibenzylamino)ethyl)-3-(3-fluoro-4-morpholinophenyl)oxazolidin-2-one (4).** White solid, yield 75%. M. P. 68.5-69.5 °C FTIR: 3059, 2955, 1753, 1514, 1449, 1402, 1234, 1117 cm^{-1}. ^1H NMR (400 MHz, $CDCl_3$): δ 7.30 (m, 10 H), 7.18 (dd, J = 11.8,

2.5 Hz, 1H), 7.00 (ddd, *J* = 7.1, 2.5, 1.0 Hz, 1H), 6.89 (dd, *J* = 9.1, 9.0 Hz, 1H), 4.40 (ddd, *J* = 8.3, 8.2, 7.2 Hz, 1H), 3.86 (m, 4H), 3.80 (t, *J* = 8.7 Hz, 1H), 3.75(d, *J* = 13.5 Hz, 2H), 3.57 (dd, *J* = 9.0, 6.6 Hz, 1H), 3.48 (d, *J* = 13.5 Hz, 2H), 3.08 (m, 4H) 2.88 (m, 1H), 1.30(d, *J* = 6.6 Hz, 3H). ^{13}C NMR (100 MHz, $CDCl_3$): δ 155.5 (d, J_{C-F} = 244.4 Hz), 154.6, 139.1, 136.2 (d, J_{C-F} = 9.0 Hz), 133.3 (d, J_{C-F} = 10.5 Hz), 128.9, 128.5, 127.4, 118.7 (d, J_{C-F} = 4.1 Hz), 114.2 (d, J_{C-F} = 3.3 Hz), 107.7 (d, J_{C-F} = 25.8 Hz), 74.2, 66.9, 56.7, 54.6, 51.9, 49.4, 8.6. HRMS (FAB$^+$) calculated for $C_{29}H_{33}FN_3O$: 490.2506. Found: 490.2513 uma.

((*S*)-5-((*S*)-1-(dibenzylamino)ethyl)-3-(3-fluoro-4-morpholinophenyl)oxazolidin-2-one (5). White solid, yield 70%. M. P. 78.0-79.0 °C. FTIR: 3032, 2955, 1753, 1514, 1449, 1402, 1234, 1117 cm^{-1}. ^{1}H NMR (400 MHz, $CDCl_3$): δ 7.37 (dd, *J* = 11.8, 2.6 Hz, 1H), 7.30 (m, 10 H), 7.00 (ddd, *J* = 7.3, 2.0, 1.3 Hz, 1H), 6.94 (dd, *J* = 9.2, 9.0 Hz, 1H), 4.56 (ddd, *J* = 5.4, 5.1, 5.1 Hz, 1H), 3.93 (d, *J* = 13.6 Hz, 2H), 3.88 (m, 4H), 3.68 (dd, *J* = 8.4, 2.4 Hz, 1H), 3.48 (d, *J* = 13.6 Hz, 2H), 3.07 (m, 4H), 2.92 (dc, *J* = 6.8, 5.1 Hz, 1H), 1.26 (d, *J* = 6.8 Hz, 3H). ^{13}C NMR (100 MHz $CDCl_3$): δ 155.5 (d, J_{C-F} = 244.5 Hz), 154.5, 139.6, 136.2 (d, J_{C-F} = 8.9 Hz), 133.5 (d, J_{C-F} = 10.5 Hz), 128.9, 128.3, 127.0, 118.7 (d, J_{C-F} = 4.2 Hz), 113.7 (d, J_{C-F} = 3.3 Hz), 107.3 (d, J_{C-F} = 26.3), 76.2, 67.0, 55.1, 54.8, 51.0, 47.6, 10.2. HRMS (FAB$^+$) calculated for $C_{29}H_{33}FN_3O$: 490.2506. Found: 490.2513.

Hydrogenolysis of 4 and 5

Compounds **4** or **5** (1 g, 2.04 mmol) were dissolved in dry methanol (25 mL) and Pd/C 10% (0.02 g, 0.20 mmol) was added. Then two drops of acetic acid were added, and the reaction mixture was stirred for 4 h under H_2 atmosphere. Then, the mixture was filtered on a Celite pad in order to remove the Pd/C, and the organic solvent was evaporated under vacuum conditions.

(*R*)-5-((*S*)-1-aminoethyl)-3-(3-fluoro-4-morpholinphenyl)oxazolidin-2-one (**6**). White solid, yield 90%. M. P. 196-197 °C. FTIR: 3373, 2952, 2835, 1740, 1636, 1514, 1445, 1404, 1237, 1112 cm^{-1}. ^{1}H NMR (400 MHz, $CDCl_3$): δ 7.50 (dd, *J* = 11.8, 2.6 Hz, 1H), 7.22 (ddd, *J* = 8.8, 1.5, 1.2 Hz, 1H), 7.08 (dd, *J* = 9.1, 9.0 Hz, 1H), 4.77 (m, 1H), 4.10 (t, *J*

= 9.3 Hz, 1H), 4.00 (m, 1H), 3.74 (m, 4H), 3.40 (m, 1H), 2.96 (m, 4H) 1.16 (d, J = 6.6 Hz, 3H). ^{13}C NMR (100 MHz, $CDCl_3$): δ 155.5 (d, $J_{C\text{-}F}$ = 220.4 Hz), 154.3, 136.2 (d, $J_{C\text{-}F}$ = 7.3 Hz), 133.6 (d, $J_{C\text{-}F}$ = 10.2 Hz), 119.7 (d, $J_{C\text{-}F}$ = 4.1 Hz), 114.8 (d, $J_{C\text{-}F}$ = 3.3 Hz), 107.3 (d, 26.1), 74.2, 66.6, 51.1, 48.7, 46.5, 14.6. HRMS (FAB$^+$) calculated for $C_{15}H_{21}FN_3O_3$: 310.1567. Found: 310.1621.

(*S*)-5-((*S*)-1-aminoethyl)-3-(3-fluoro-4-morpholinophenyl)oxazolidin-2-one (7). White solid, 80% yield. M. P. 128-129 °C. FTIR: 3373, 2956, 1744, 1625, 1514, 1407, 1234, 1114 cm^{-1}. ^{1}H NMR (400 MHz, $CDCl_3$): δ 7.51 (dd, J = 12.4, 2.6 Hz, 1H), 7.23 (dd, J = 8.8, 1.9 Hz, 1H), 7.05 (dd, J = 9.8, 9.1Hz, 1H), 4.45 (ddd, J = 8.7, 8.6, 7.8 Hz, 1H), 4.01 (dd, J = 9.0, 8.9 Hz, 1H), 3.83 (dd, J = 9.0, 8.9 Hz, 1H), 3.73 (m, 4H), 3.25 (bs, 2H), 2.96 (m, 5H), 1.03 (d, J = 6.5 Hz, 3H). ^{13}C NMR (100 MHz, $CDCl_3$): δ 155.5 (d, $J_{C\text{-}F}$ = 242.1 Hz), 154.7, 135.8 (d, $J_{C\text{-}F}$ = 8.8 Hz), 134.1 (d, $J_{C\text{-}F}$ = 10.4 Hz), 119.7 (d, $J_{C\text{-}F}$ = 4.2 Hz), 114.4 (d, $J_{C\text{-}F}$ = 3.2 Hz), 107.3 (d, $J_{C\text{-}F}$ = 26.0Hz), 75.8, 66.6, 51.2, 49.2, 47.1, 18.2. HRMS (FAB$^+$) calculated for $C_{15}H_{21}FN_3O_3$: 310.1567. Found: 310.1621.

*N-acetylation of **6** and 7*

To a solution of **6** or **7** (1 g, 3.23 mmol) in dry dichloromethane (50 mL), TEA (0.1 mL, 6.5 mmol) was added dropwise at -78 °C under argon atmosphere and the mixture was stirred for 15 min. Then a solution of acetyl chloride (0.38 g, 4.85 mmol) in 5 mL of solvent was added dropwise, and the reaction was stirred for 45 min at the same temperature. Then the organic layer was washed with brine, separated, dried over Na_2SO_4 and filtered. The solvent was evaporated under reduced pressure.

***N*-((*S*)-1-((*R*)-3-(3-fluoro-4-morpholinphenyl)-2-oxooxazolidin-5-il)ethyl)acetamide (8).** Yellow solid, 76% yield. M. P. 140-142 °C. FTIR: 3323, 3063, 2920, 1741, 1659, 1514, 1220 cm^{-1}. ^{1}H NMR (400 MHz, $CDCl_3$): δ 7.45 (dd, J = 15.0, 2.5 Hz, 1H), 7.13 (dd, J = 9.1, 2.5 Hz, 1H), 6.93 (t, J = 9.2 Hz, 1H), 6.02 (d, J = 8.4 Hz, 1H), 4.70 (m, 1H), 4.25 (m, 1H), 4.08 (t, J = 9.1 Hz, 4H), 3.88 (m, 4H), 3.78 (dd, J = 9.0, 8.8 Hz, 1H), 3.04 (m, 4H), 2.00 (s, 1H), 1.25 (d, J = 7.0 Hz, 3H). ^{13}C NMR (100 MHz, $CDCl_3$): δ 169.9, 155.0

(d, J_{C-F} = 242.2 Hz), 154.4, 136.5 (d, J_{C-F} = 8.8 Hz), 132.8 (d, J_{C-F} = 10.5 Hz), 118.7 (d, J_{C-F} = 4.1 Hz), 114.0 (d, J_{C-F} = 3.0 Hz), 107.5 (d, J_{C-F} = 26.0Hz), 74.4, 66.9, 51.0, 47.7, 47.6, 23.2, 13.4. HRMS (FAB^+) calculated for $C_{17}H_{23}FN_3O_4$: 352.1673. Found: 352.1705.

***N*-((*S*)-1-((*S*)-3-(3-fluoro-4-morpholinphenyl)-2-oxooxazolidin-5-il)ethyl)acetamide (9).** White solid, 70% yield. M. P. 196-198 °C. FTIR: 3323, 3063, 2920, 1741, 1659, 1514, 1220 cm^{-1}. ^1H NMR (400 MHz, $CDCl_3$): δ 7.42 (dd, *J* = 15.0, 2.5 Hz, 1H), 7.05 (dd, *J* = 8.8, 2.5 Hz, 1H), 6.90 (dd, *J* = 9.26, 9.0 Hz, 1H), 6.41 (d, *J* = 8.0 Hz, 1H), 4.60 (m, 1H), 4.45 (m, 1H), 3.94 (t, *J* = 9.0 Hz, 4H), 3.88 (m, 5H), 3.05 (m, 4H), 1.97 (s, 1H), 1.35 (d, *J* = 7.0 Hz, 3H). ^{13}C NMR (100 MHz, $CDCl_3$): δ 170.9, 155.4 (d, J_{C-F} = 245.0 Hz), 154.6, 136.4 (d, J_{C-F} = 8.7 Hz), 132.8 (d, J_{C-F} = 10.5 Hz), 118.7 (d, J_{C-F} = 4.2 Hz), 113.9 (d, J_{C-F} = 3.0 Hz), 107.5 (d, J_{C-F} = 26.0Hz), 75.6, 66.9, 51.0, 47.6, 46.2, 22.1, 17.8. HRMS (FAB^+) calculated for $C_{17}H_{23}FN_3O_4$: 352.1673. Found: 352.1705.

2.2 Antibacterial activity of Linezolid analogues

The antibacterial activity of all molecules was evaluated against twelve bacterial strains (eleven Gram-positive and one Gram-negative, see Table S7).[25-27] All bacteria were cultured in Muller-Hinton broth. MIC of all compounds were determined by broth microdilution method according to CLSI guidelines. The 18-20 h grown culture gives about 10^8 CFU/mL of bacteria. The bacterial cultures were diluted to give approximately 10^6 CFU/mL in Muller-Hinton broth media and then were used to determinate antibacterial activity.

The evaluation of the antibacterial activity of all compounds against different Gram-positive and Gram-negative strains was performed at 100 μg/mL into 96-wells ELISA type dishes. Then, the active compounds were evaluated at lower concentration in the range of 50 to 1.17 μg/mL.

2.3 In vitro antiparasitic activity of Linezolid analogues

Antiparasitary evaluations were made at one concentration that corresponds to the Praziquantel solubility (20 mg/mL) in Hank's medium. *Hymenolepis nana* worms were

exposed to Linezolid analogues or Praziquantel (positive control) in 24-well sterile plates, 5 worms/well in 1 mL of medium. Parasites in Hank's medium were used as negative control. The plates were monitored by light microscope every hour up to 12 h and then every 24 h up to 72 h; morphology, mobility and vitality were registered.[28] Concentration-response assays of selected Linezolid analogues (10, 15 and 20 mg/mL) on the antiparasitic activity were performed.

2.4 Cellular viability assay

Insight about the effect of the linezolid analogues **6** to **9** on cell proliferation, cell viability was assessed on human retinal pigment epithelial cell line (ARPE-19) by MTT assays[29] with some modifications.[30] ARPE-19 (CRL-2302) were purchased from American Type Culture Collection (ATCC). Initially, ARPE cells (1×10^4 per well, 50 µL) maintained in DMEM (Sigma-Aldrich) supplemented with 5% FBS (Gibco®, Thermo Fisher Scientific), were placed in each well of a 96-well plate (Costar®, USA). The analogues were dissolved in dimethyl sulfoxide (DMSO) at 40 mM. After 24 h of incubation at 37 °C in a 5% CO_2 atmosphere to allow cells attachment, aliquots (50 µL) of the medium containing different concentrations (12.5 to 400 µM) of linezolid analogues were added to cell cultures, and were incubated for 48 h. We used the cytotoxic drug Doxorubicin hydrochloride (Sigma-Aldrich) as a positive control in cellular viability assays. In the last 4 h of each assay, 10 µL of an MTT (Thiazolyl Blue Tetrazolium Bromide; Sigma-Aldrich) solution (5 mg/mL) were added to each well. The cell viability was calculated by the ability of metabolically active cells to reduce tetrazolium salt formazan. The formazan crystals were dissolved with acidic isopropyl alcohol (0.3 %). The OD was measured on a microplate reader (Multiskan EX, ThermoLabSystem) using a test wavelength of 570 nm and a reference wavelength 630 nm. The effect over cell viability of linezolid analogues was reported as a proliferation percentage to each concentration evaluated.

3. Results and discussion

3.1 Chemistry

Oxazolidinones **1** and **2** were prepared following a methodology previously reported in 90 and 84% global yield.[21,22] Compound **3** was obtained starting by a nucleophilic aromatic substitution reaction of 3,4-difluoronitrobenzene and morpholine in a 90% yield. Then, the nitro group was reduced under a H_2 atmosphere using the Pd/C catalyst to obtain the amino derivate in 97% yield. The amino group was exchange by a bromine with a 80% yield under a Sandmeyer reaction conditions (Scheme S1).[23,24] Aryl coupling of **3** with oxazolidinones **1** and **2** leaded to *N*,*N*-dibenzylamine Linezolid analogues **4** and **5** in 75 and 70% yield, respectively. Then, a hydrogenolysis reaction allowed the synthesis of amino-free derivates **6** and **7** in 90 and 80% yield. Finally, compounds **6** and **7** were acetylated to form **8** and **9** in 70 and 76% yield, respectively (Scheme 1). Analogues **8** and **9** have high estructural resemblance to Linezolid, but with two significant differences, their molecules have two chiral centers and a methyl group attached to the acetamide methyl substituent.

Scheme 1. Synthetic route for the preparation of Linezolid analogues.

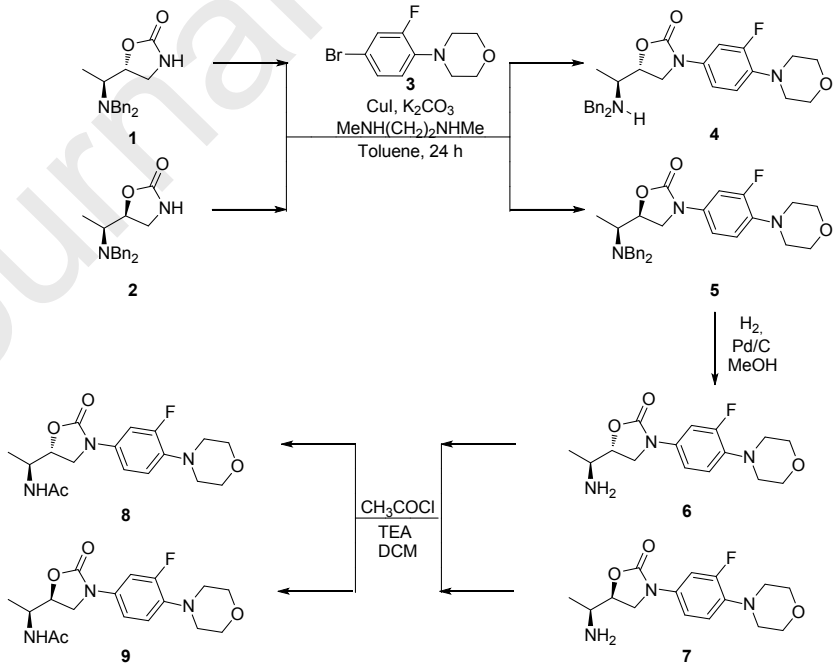

All compounds were characterized by FTIR, ^{1}H and ^{13}C NMR, and mass spectrometry. ^{1}H NMR spectrum of oxazolidinone **1** shows the characteristic signals of benzyl groups at 7.30 ppm for aromatic hydrogens, and at 3.75 and 3.47 ppm two doublets assigned to methylene hydrogens. There is a broad singlet at 5.46 ppm belonging to carbamate hydrogen and a multiplet at 4.50 ppm assigned to oxazolidinone methine. The signals for oxazolidinone methylene hydrogens appear as two triplets located at 3.58 and 3.25 ppm. The signal of alanine methine (asymmetric center) is present at 2.86 ppm and there is a doublet signal located at 1.26 assigned to methyl hydrogens (Figure S1). The oxazolidinone carbonyl signal appears at 159.6 ppm in the ^{13}C NMR spectrum of **1**. There are four aromatic signals from 139.3 to 127.3 ppm and benzylic methylene signal is located at 54.6 ppm. The oxazolidinone methine and methylene signals are observed at 78.5 and 44.8 ppm, respectively. The signal of alanine asymmetric carbon is located at 56.7 ppm and methyl carbon at 8.7 ppm (Figure S2). A stretching vibration band for carbonyl is located at 1746 cm^{-1} in the FTIR spectrum (Figure S3). The MS(ESI) analysis of **1** shows the quasimolecular ion $[M+H]^{+}$ with 311 amu and adducts $[M+Na]^{+}$ and $[M+K]^{+}$ with 333 and 349 amu, respectively (Figure S4). The NMR spectra of **2** show the same signals than **1**, but slight differences in their chemical shifts are observed due to the different configuration at C5 position (Figures S5 and S6). Oxazolidinone **1** crystallized as a dimer in the monoclinic crystalline system with a space group $P2_1$ (Figure 2 and Table S1). Interestingly, the asymmetric unit of **1** showed two oxazolidinone molecules connected to each other by hydrogen bonding of oxazolidinone unit. These two intermolecular hydrogen bonds (NH···O=C) have been described as a strong non-covalent interaction with Donor···Acceptor distances of 2.889 and 2.939 Å.[31]

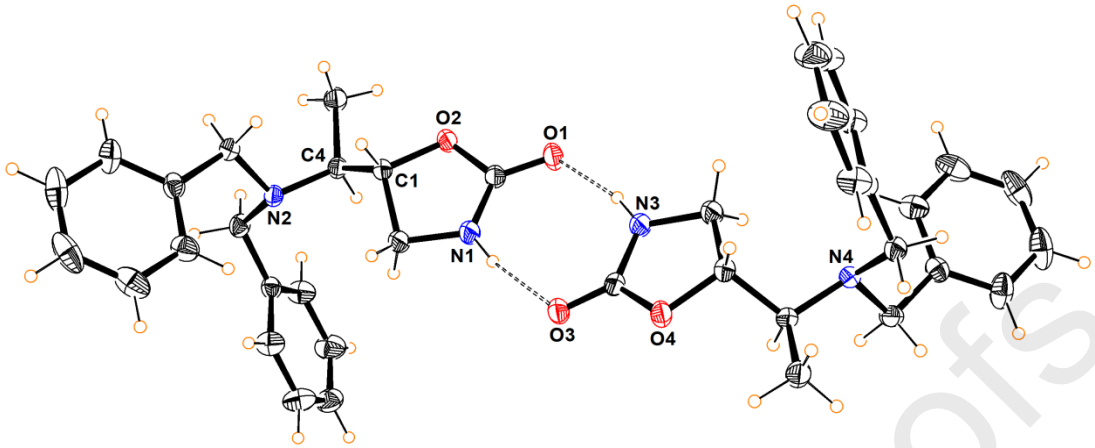

Figure 2. Dimeric molecular structure of compound **1** with thermal ellipsoids drawn at 20% probability level. Bond distances of the non-covalent interactions D···A (Å): N(3)···O(1)=C, 2.939(4); N(1)···O(3)=C, 2.889(4).

In addition, the hydrogens of chiral carbons (C1 and C4) have an *anti*-conformation with an *R* and *S* absolute configuration on C1 and C4, respectively (Flack parameter = 0.05(8). The crystal arrangement exhibits intermolecular C–H···O hydrogen bonds, which together with the intermolecular hydrogen bonds of the type NH···O=C, led to formation of the 2D framework (Figure S7).

The ^{1}H NMR spectrum of **3** shows a multiplet at 7.26 ppm and a triplet a 6.89 ppm corresponding to aromatic hydrogens. There are two multiplets at 3.87 and 3.07 ppm belonging to morpholine fragment (Figure S8). Some aromatic signals located at 156.7 to 113.9 ppm in the ^{13}C NMR spectrum present a doublet multiplicity due to coupling with fluorine. The characteristic signal for the *ipso* fluorine carbon is located at 155 ppm with a *J*= 249.3 Hz. The aliphatic carbons are located at 66.9 and 50.8 ppm, respectively (Figure S9). In addition, it was possible to obtain the X ray crystal structure of **3** (Figure 3, Table S2) and its synthetic precursors **12** and **13** (Figure S10, Tables S3 and S4), which have not been published. The molecular structure of **3** and its precursors have morpholine ring in a chair-conformation with nitrogen substituted at the equatorial position by the aryl group (Figure 3). The crystal arrangement exhibits intermolecular C–H···F and C–H···O hydrogen bonds in compound **3**. Moreover, the crystal of **3** presents one π-π interaction between the phenyl rings of two molecules (Figure S11).

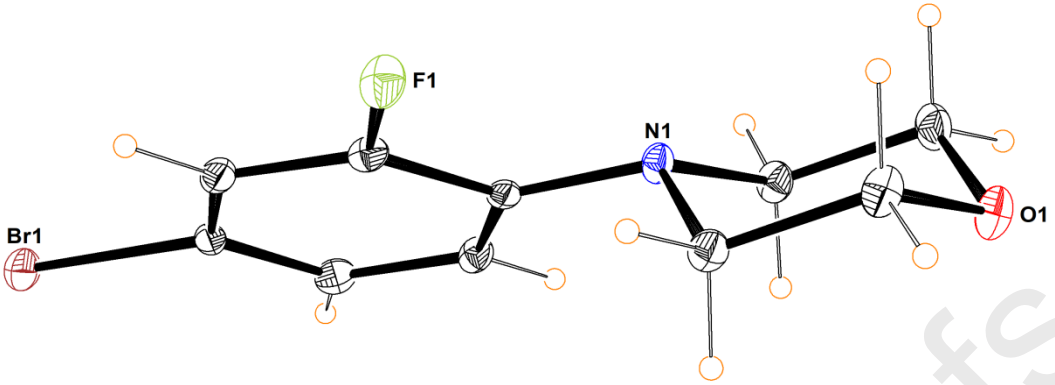

Figure 3. Molecular structure of compound **3** with thermal ellipsoids drawn at 50% probability level.

^{1}H NMR spectra of **4** and **5** show signals corresponding to both oxazolidinone and fluorophenylmorpholine moieties, with significant differences in the chemical shift of oxazolidinone methylene and fluorophenyl hydrogens. The rest of signals have similar chemical shifts to their respective precursors (Figures S12 and S14). Similarly, all carbon signals belonging to both fragments are presented, but significant differences in the chemical shift of oxazolidinone carbons C4 and C5, morpholine C14 and fluorophenyl C8 signals are observed, due to the coupling of both fragments (Figures S13 and S15). The FTIR spectra of **4** and **5** show a stretching band for carbonyl at 1744 cm^{-1} (Figure S16). The MS(ESI) analysis of these compounds show a quasimolecular ion $[M+H]^+$ with 490 amu and the adduct $[M+Na]^+$ with 512 amu (Figure S17).

Signals belonging to benzylic groups are no longer present in the ^{1}H NMR spectra of **6** and **7**, and oxazolidinone signals are shifted downfield (Figures S18 and S20). Only the fluorphenyl signals are present in the aromatic zone in ^{13}C NMR spectra, the rest of aliphatic carbon signals have different chemical shift (Figures S19 and S21). FTIR spectra show the amino-group stretching vibrations at 3384 y 3365 cm^{-1}, and carbonyl stretching at 1734 cm^{-1} (Figure S22). The MS(ESI) analysis show a quasimolecular ion $[M+H]^+$ with 310 amu corresponding to these compounds (Figure S23).

^{1}H NMR spectra of acetylated derivates **8** and **9** present two new signals due to the acetyl group. There is a doublet at 6 ppm and a singlet at 2 ppm assigned to amide and a methyl

hydrogens, respectively. The chemical environment of the rest of hydrogens was affected by the presence of acetyl group, particularly the H6 signal shifted 0.8 and 1.4 ppm in **8** and **9**, respectively (Figures S24 and S26). ^{13}C NMR spectra show the new carbonyl and methyl signals at 170 and 23 ppm, respectively (Figures S25 and S27). There are two new stretching bands at 3275 and 1647 cm^{-1} in FTIR spectra due to the presence of acetyl group in these molecules (Figure S28). The MS(ESI) analysis of **8** and **9** shows a quasimolecular ion $[M+H]^+$ with 352 amu, and adducts $[M+Na]^+$ and $[M+K]^+$ with 374 and 391 amu, respectively (Figure S29). Figure 4 shows the sequence of ^1H NMR spectra obtained from the oxazolidinone **1** to Linezolid analogue **8**. A full assignation of NMR signals is summarized in Tables S5 and S6.

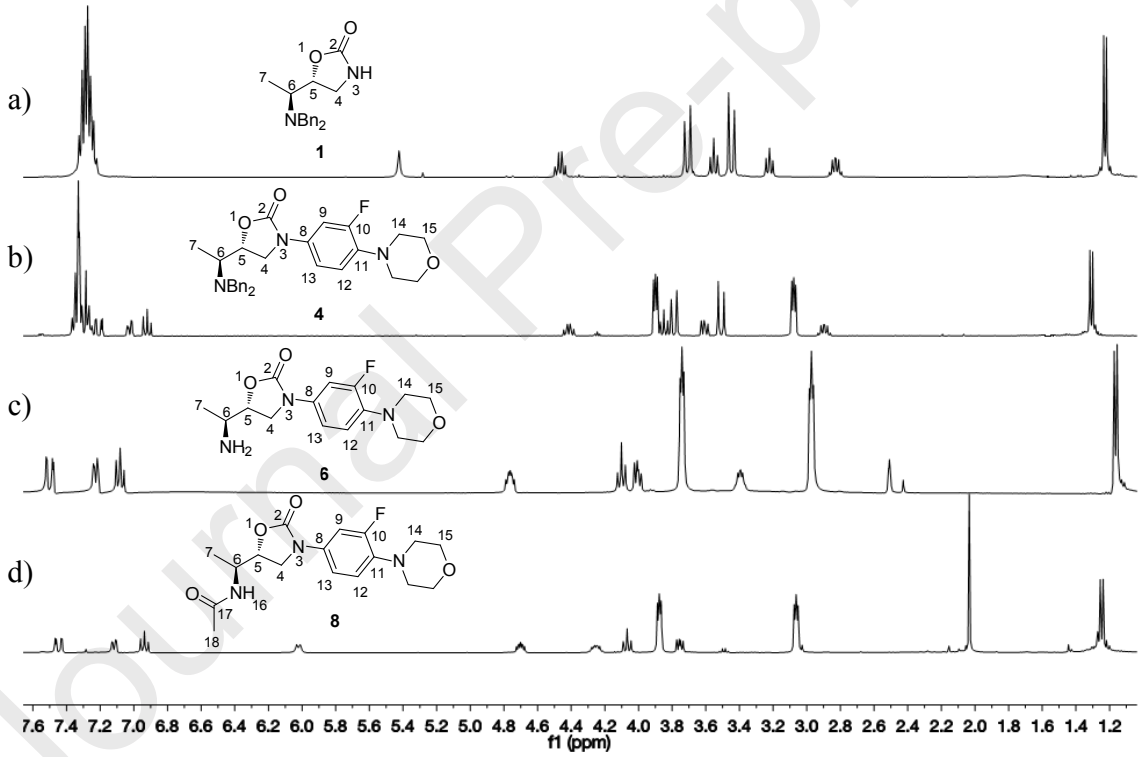

Figure 4. Partial ^1H NMR spectra of **1** (a), **4** (b), **6** (c) and **8** (d).

3.2 In vitro activity of Linezolid analogues against bacterial strains

First, the antibacterial activity of dibenzylamino oxazolidinones **1** and **2**, and Linezolid analogues **4-9** was evaluated against Gram-positive and Gram-negative strains (Table S7) at 100 μg/mL. Linezolid was evaluated as positive control against the same strains. The

active compounds at this concentration were **1**, **2**, **5** and **6**, only against Gram positive strains. Dibenzylamino oxazolidinone **1** was active against group A *Streptococcus* 01 and ATCC 25923 *Staphylococcus aureus* and dibenzylamino oxazolidinone **2** was active against group A *Streptococcus* 01, *Staphylococcus aureus* 05, ATCC 25923 *Staphylococcus aureus*, MRSA-01, MRSA-03 and MRSA-05. Linezolid analogues **5** and **6** were active against *Staphylococcus aureus* 05.

Then, their antibacterial activity was evaluated at lower concentration in the range of 1.17 to 50.0 μg/mL. The results showed that at lower concentration these compounds do not display activity against all the initial strains. Dibenzylamino oxazolidinones **1** and **2** only inhibited the growing of group A *Streptococcus* 01 strain, but a small bacterial button was observed even at the highest concentration (50.0 μg/mL) and the Linezolid analogues **5** and **6** showed activity only against *Staphylococcus aureus* 05 at 50 μg/mL.

The experimental results demonstrated the poor antibacterial activity of these Linezolid analogues compared to Linezolid (Table S8). In order to rationalize this significant difference in the antibacterial activity at the molecular level, the molecular docking of Linezolid analogues **4**-**9** in the Phosphoryl Transferase Center (PTC) of Linezolid was done using the MOE 2018[32] program. The docking was performed with the crystallographic structure of ribosomal RNA (rRNA) of *E. coli* (Proten Data Bank ID: 4V4Q) with the same protocol previously reported for another Linezolid analogues.[33] The structure of all Linezolid analogues, excepting **4**, occupy the PTC of *E. coli* (Figures S30 to S36).[34] The protonated forms of **6** and **7** were also calculated. Table 1 shows the score and placement energies (in kcal/mol) of Linezolid and analogues. The score value obtained after several calculations is related to the quality of the coupling, where the lower scores indicate the most favorable couplings. As can be seen, analogues **5**, **6** and **8** have similar score than Linezolid, but they do not show potent antibacterial activity as Linezolid. Some plausible reasons for this difference could be: 1) a highly superior placement energy to Linezolid, probably due to the steric effect of voluminous groups as benzyl or methyl present in their molecular structure, and 2) different intermolecular interactions involved in the supramolecular complexes. The docking of Linezolid in the PTC of *E. coli* shows the

typical hydrogen bond interaction between the amide hydrogen and the phosphodiester group of G2505 nucleotide, which is the main interaction responsible of the antibacterial activity.[35] Linezolid analogue **5** presents a non-typical hydrogen bond with the G2061acting as H-acceptor, while analogue **6** presents two interactions, one hydrogen bond with G2505 acting as H-donor and a lower energy C-H···π interaction with A2451 (Figure 5). These analogues display poor activity against one bacterial strain. The rest of Linezolid analogues which are totally inactive establish low energy interactions such as C-H···π and N-H···π, but no hydrogen bonds are present (Figures S30 to S36).

Table 1. Score and placement energy (kcal/mol) of Linezolid analogues.

Compound	Score (kcal/mol)	Placement Energy (kcal/mol)
Linezolid	-7.20	-70.35
5	-7.18	-9.27
6-H$^+$	-5.85	-41.51
6	-7.18	-53.12
7-H$^+$	-6.28	-46.24
7	-6.69	-39.42
8	-7.19	-54.64
9	-6.88	-53.92

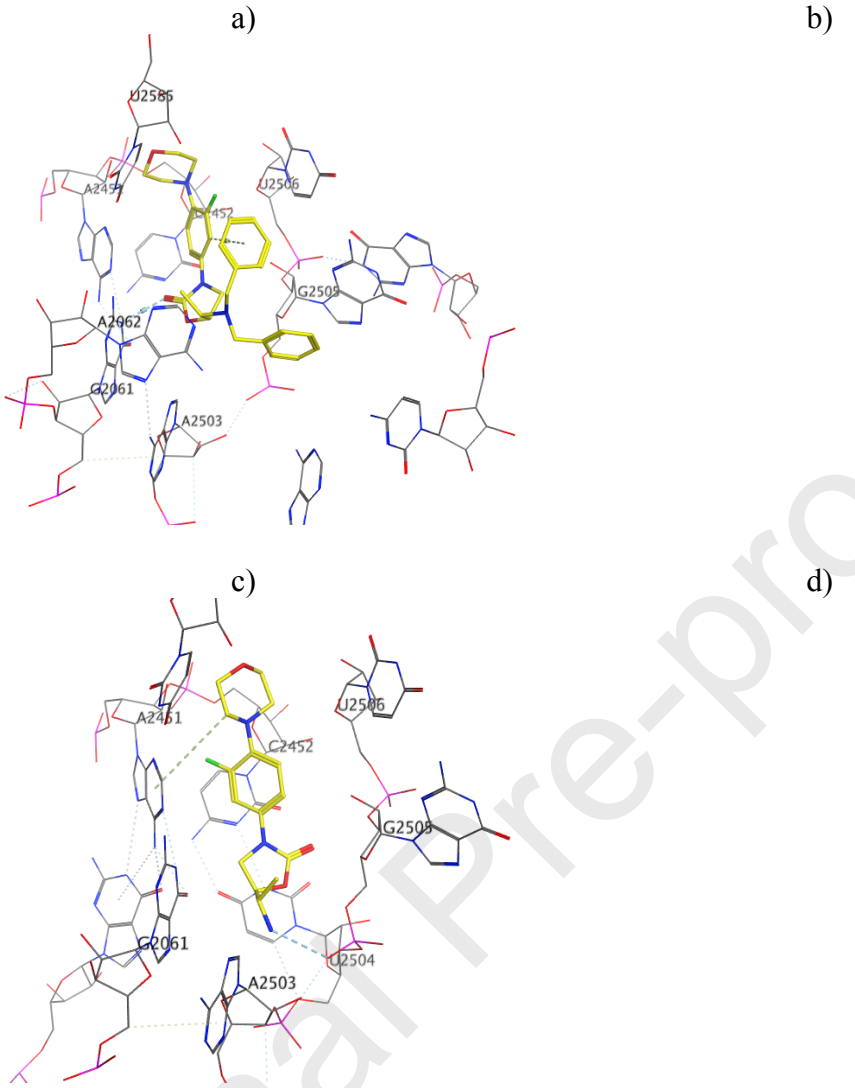

Figure 5. Molecular docking and interaction maps of **5** (a and b) and **6** (c and d) with the Phosphoryl Transferase Center (PTC) of the crystallographic structure of ribosomal RNA (rRNA) of *E. coli*.

3.3 In vitro activity of Linezolid analogues against *Hymenolepis nana*

Based on results obtained in the antibacterial experiments, it was decided to evaluate the *in vitro* antiparasitic activity of Linezolid analogues **4-9** against *H. nana* at 20 mg/mL following a procedure previously reported by Montes-Ávila.[28] The study consists of observing the parasite mobility and morphology in the presence of Linezolid analogue, as well as its viability using the Evans staining. Analogues **4** and **5** induced paralysis and death at 20 and 60 min, respectively (Table 2). Death time was twice that observed with

Praziquantel (30 min), but interestingly, compounds **4** and **5** cause morphological damage to the parasite's scolex, neck and proglottids (Figure 6b). Analogues **6** and **7** have a similar time of paralysis (11 and 10 min, respectively) and death time (21 min). Both compounds showed higher potency than Praziquantel. The staining showed morphological damage to the gravid proglottids, scolex and eggs caused by **6** (Figure 6c). These effects in the parasite were not observed with Praziquantel and they are important due to the parasitosis persistence is associated with the scolex attachment to the intestine and with the reinfection by the eggs present in the gravid proglottids.[36] Based on these results, the chemical configuration in **4** and **5** does not have effect over the antiparasitic activity, as well as in **6** and **7**. Paralysis and death times were similar with these diasteromeric pairs. Instead, analogues **8** and **9** had significant differences in activity, the death time observed with **8** was three-times that of **9**. Analogue **9** was the most active Linezolid analogue against *H. nana* with a death time of almost half (18 min) found with Praziquantel (30 min). More details of the anatomic damage caused by these compounds in the parasite are provided in Table 2. Linezolid only caused a reversible paralysis in the worms, there was not anatomic damage and the parasite was alive even after 24 h of treatment.

Table 2. Antiparasitic activity of Linezolid analogues against *Hymenolepis nana* at 20 mg/mL.

Compound	Structure	Paralysis (min)	Death (min)	Anatomic effect
4	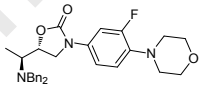	20	60	Partial staining, damage in gravid proglottids, moderate release of unstained eggs
5	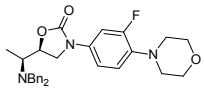	20	60	Partial staining, damage in neck, scolex and mature proglottids
6	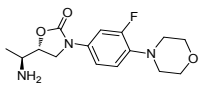	11	21	Total staining, damage in the gravid proglottids, scolex and release of stained eggs
7	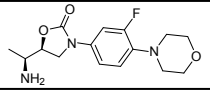	10	21	Total staining

8	2	60	Partial staining, damage in neck, scolex and mature proglottids
9	6	18	Total staining
Praziquantel	20	30	Total staining
Linezolid	5	N/D	Reversible paralysis, no anatomic damage
Control (-)	N/D	N/D	Normal mobility, no anatomic damage

N/D indicates that parasites were still moving or alive up to 16 h.

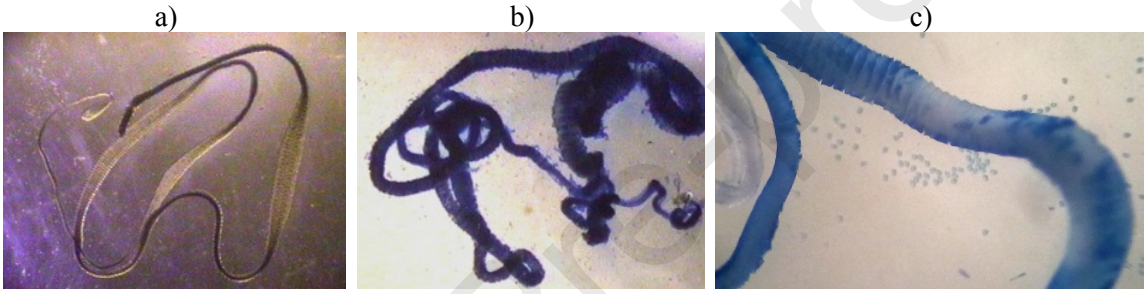

Figure 6. Pictures of *H. nana* worms a) without treatment, b) treated with **4** for 1 h and c) treated with **6** for 20 min.

Antiparasitic activity of the most active analogues **6** to **9** was study at 20, 15 and 10 mg/mL (Table 3). Paralysis and death times gradually increase at lower concentrations but, with exception of **8**, the antiparasitic activity of Linezolid analogues was preserved. Interestingly, analogues **7** and **9** (*S*,*S* stereoisomers) were more active than **6** and **8** (*R*,*S* stereoisomers). In fact, the activity of **8** diminished considerably at lower concentration. The most active analogues at lower concentration were **6** and **7**. Several factors may be considered in the antiparasitic activity of these compounds, but the solubility in aqueous media plays an important role. Amino-free (**6** and **7**) and acetylated (**8** and **9**) analogues have higher solubility than **4** and **5**, enhancing the availability to interact with the parasite.

Table 3. Antiparasitic activity of Linezolid analogues against *Hymenolepis nana* at different concentration.

Compound	Structure	Concentration (mg/mL)	Time	
			Paralysis (min)	Death (min)
6	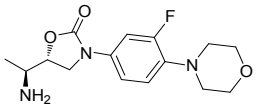	10	20	120
		15	15	40
		20	11	21
7	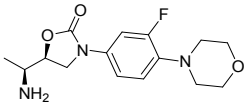	10	15	60
		15	10	60
		20	10	21
8	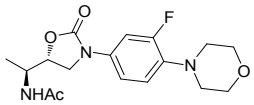	10	10	N/D
		15	10	N/D
		20	2	60
9	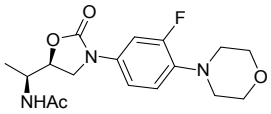	10	10	90
		15	10	90
		20	6	18

N/D indicates that parasites were still moving or alive up to 16 h.

Considering the paralysis effect of Linezolid and its analogues over the parasite, it is possible that their mechanism of action being the same as Praziquantel, that is, the alteration of the Ca^{2+} ions flux through the cell membrane caused by the interaction of these compounds into the ions channels. In this regard, it is important to point out that although Praziquantel and Linezolid do not have a similar structure, they share some similitudes such as having an aromatic group, a heterocyclic ring and an exocyclic carbonyl group, which presumably establish similar intermolecular interactions. On the other hand, the potent activity and morphological damage showed by the Linezolid analogues may be consequence of a stronger interaction due to the additional chiral center, as well as the bulky groups present in their structures inducing conformational and tridimensional arrangements favoring their interaction into the ions channels.

3.4 Cellular viability assay

In order to evaluate whether the Linezolid analogues (**6-9**) induce changes over proliferation profile of ARPE-19 cells, their effect on cell viability was evaluated by MTT assay after 48 h of treatment.[29,30] None of the analogues significantly affected the cell viability at any concentration tested (50, 100, 200 and 400 μM) (Figure S37). After 48h treatment, Linezolid analogues decreased cell proliferation between 5-20%, approximately, at the highest concentration evaluated (400 μM), in comparison with DMSO dissolvent control (Table 4). Unlike, Doxorubicin induced a strong antiproliferative effect over ARPE-19 cells and reduces the cell proliferation in a 30% at 0.2 μM.

Table 4. Proliferation percentages of ARPE-19 cells culture with Linezolid analogues at the highest concentration tested (400 μM)

Compound	Structure	Proliferation %[a]
6	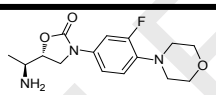	76.5 ± 1.7
7	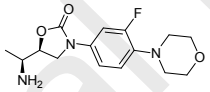	85.2 ± 1.0
8	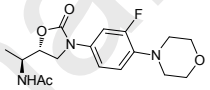	94.9 ± 1.2
9	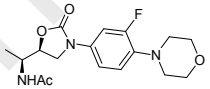	89.9 ± 2.3
Linezolid	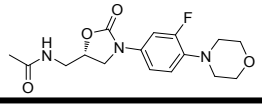	83.1 ± 4.3[c]

[a] Data is expressed as mean of three independent experiments performed by triplicate.

[b] Doxorubicin was employed as a control.

[c] Evaluated at 100 μM.

ARPE-19 cells not only remained metabolically active after the treatment, but also maintained their cellular integrity, indicating non-cytotoxic effects of Linezolid analogues (Figure S38).

Finally, important molecular properties such as $LogP_{ow}$, H-donor and H-acceptor number, molecular weight (MW), knowing as Lipinki's rule or the rule of 5,[37,38] and total polar surface area (TPSA) were calculated. The results predict these Linezolid analogues might have good permeability after orall administration (Table S14).

4. Conclusions

Herein, we present the first Linezolid type compounds reported with *in vitro* antiparasitic activity against *Hymenolepis nana*. The biological evaluations demonstrate their promising potential as antiparasitic agents because they are more active and induce anatomic damages not observed with Praziquantel, a common drug used in the treatment of this parasitosis. Noteworthy, the newly synthesized Linezolid analogues preserve the cellular integrity and metabolic viability of ARPE-19 cells indicating no *in vitro* cytotoxic affects. These Linezolid analogues may represent a new therapeutic alternative for treatment of the disease cause by *H. nana*. Further studies will be conducted to study the activity of these compounds against other intestinal parasites.

5. Acknowledgements

Authors thank to Consejo Nacional de Ciencia y Tecnología (CONACYT) for the financial support for these research (Grant No. SALUD-2015-1-261324), Supramolecular Chemistry Thematic Network (Grant No. 294810), NMR facilities (Grant INFR-2011-3-173395), X ray facilities (Grant INFR-2014-224405) and the scholarship program, which supported to Eleazar Alcántar-Zavala and Esteban Hernández-Guevara for their postgraduate studies. The docking software MOE was support by the Instituto de Investigaciones Biomédicas at the UNAM, through the program "Novel alternatives for the Treatment of Infection Deseases (NUATEI-IIB-UNAM)" and the program "Apoyo a la Investigación y el Posgrado (PAIP)" Grant 5000-9163 in the Chemistry Faculty of the UNAM.

6. Supplementary information

FTIR, ^{1}H and ^{13}C NMR spectra are provided in a Supplementary Material File. All crystallographic were deposited in the Cambridge Crystallographic Data Centre and the accession numbers are 1958671, 1960623, 1960624 and 1960627.

7. References

1.- Langbang, D.; Dhodapkar, R.; Parija, S. C.; Premarajan, K. C. Rajkumari, N. Prevalence of intestinal parasites among rural and urban population in Puducherry, South India - A community-based study. *J. Family Med. Prim. Care* **2019**, *8*, 1607-1612. doi:10.4103/jfmpc.jfmpc_196_19

2.- Yang, D.; Zhao, W.; Zhang, Y.; Liu A. Prevalence of *Hymenolepis nana* and *H. diminuta* from Brown Rats (*Rattus norvegicus*) in Heilongjiang Province, China. *Korean J. Parasitol*. **2017**, *55*, 351-355. doi:10.3347/kjp.2017.55.3.351

3.- Shahnazi, M.; Mehrizi, M. Z.; Alizadeh, S. A.; Heydarian, P.; Saraei, M.; Alipour, M.; Hajialilo, E. Molecular characterization of *Hymenolepis nana* based on nuclear rDNA ITS2 gene marker. *Afr. Health Sci*. **2019**, *1*, 1346-1352. doi:10.4314/ahs.v19i1.6

4.- López-Angulo, G.; Verdugo-Gaxiola, S. E.; Montes-Avila, J.; Díaz-Camacho, S. P.; Miranda-Soto, V.; Salazar-Salas, N. Y.; Delgado-Vargas, F. Bioguided isolation of *N*-malonyl-(+)-tryptophan from the fruit of *Pithecellobium dulce* (Roxb.) Benth. that showed high activity against *Hymenolepis nana*. *Nat. Prod. Res.* **2019**, *33*, 1-7. doi:10.1080/14786419.2019.1590709

5. Kandi V.; Koka S. S.; Bhoomigari, M. R. Hymenolepiasis in a Pregnant Woman: A Case Report of *Hymenolepis nana* Infection. *Cureus* **2019**, *11*, e3810. doi:10.7759/cureus.381

6. Ahmed, O.; Elmesallamy, Gel-S.; Eassa, S. Comparative study of the hepatotoxic, genotoxic and carcinogenic effects of praziquantel distocide and the natural myrrh extract Mirazid on adult male albino rats. *J. Egypt. Soc. Parasitol.* **2005**. 35, 313-29.

7. Doenhoff, M. J.; Cioli, D.; Utzinger, J. Praziquantel: mechanisms of action, resistance and new derivatives for schistosomiasis. Current Opinion in Infectious Diseases **2008**, *21*, 659-667. doi:10.1097/QCO.0b013e328318978f

8. Jeziorski, M. C.; Greenberg, R. M. Voltage-gated calcium channel subunits from platyhelminths: Potential role of praziquantel action. *Int. J. Parasitol.* **2006**, *36*, 625-636. doi:10.1016/j.ijpara.2006.02.002.

9. Ford, C. W.; Zurenko, G. E.; Barbachyn, M. R. The discovery of Linezolid, the first oxazolidinone antibacterial agent. Curr. *Drug Targets Infect. Disord.* **2001**, *2*, 181-199. doi:10.2174/1568005014606099

10. Hashemian, S. M. R.; Farhadi, T.; Ganjparvar, M. Linezolid: a review of its properties, function, and use in critical care. *Drug Des. Dev. Ther.* **2018**, *12*, 1759-1767. doi:10.2147/dddt.s164515

11. Saager, B.; Rohde, H.; Timmerbeil, B. S. Molecular characterization of Linezolid resistance in two vancomycin-resistant (VanB) *Enterococcus faecium* isolates using Pyrosequencing. *Eur. J. Clin. Microbiol. Infect. Dis.* **2008**, *27,* 873-878.

12. Besier, S.; Ludwig, A.; Zander, J.; Brade, V.; Wichelhaus, T. A. Linezolid resistance in *Staphylococcus aureus*: gene dosage effect, stability, fitness costs, and cross-resistances. *Antimicrob. Agents Chem.* **2008**, *52*, 1570-1572. doi:10.1128/aac.01098-07

13. Walked, J. A.; O′Donnell, R.; Wiener, R. S. Linezolid *vs* glycopeptide antibiotics for the treatment of suspected methicillin-resistant *Staphylococcus aureus* nosocomial pneumonia: a meta-analysis of randomized controlled trials. *Chest* **2011**, *139*, 1148-1155. doi:10.1016/j.yccm.2012.01.031

14. Zhao H.; Lu Y.; Sheng L.; Yuan Z.; Wang B.; Wang W.; Li Y.; Ma C.; Wang X.; Zhang D.; Huang H. Discovery of fluorine-containing benzoxazinyl-oxazolidinones for the treatment of Multidrug Resistant Tuberculosis. *ACS Med. Chem*. Lett. **2017**, *8*, 533−537. doi:10.1021/acsmedchemlett.7b00068

15. Leach. K. L.; Swaney, S. M.; Colca, J. R. McDonald, W. G.; Blinn, J. R.; Thomasco, L. M.; Gadwood, R. C.; Shinabarger, D.; Xion, L; Mankin, A. S. The site of action of oxazolidinone antibiotics in living bacteria and in human mitochondria. *Mol*. *Cell*. **2007**, *26*, 393-402. doi:10.1016/j.molcel.2007.04.005

16. Ippolito, A. J.; Kanyo, F. Z.; Wang, D.; Franceschi, J. F.; Moore, B. P.; Steitz, A. T; Duffy, M. E. Crystal structure of the oxazolidinone antibiotic Linezolid bound to the 50S ribosomal subunit. *J. Med. Chem*. **2008**, *51*, 3353-3356. doi:10.1021/jm800379d

17. Ferrazzano, L.; Viola, A.; Lonati, E.; Bulbarelli, A.; Musumeci, R.; Cocuzza, C.; Lombardo, M.; Tolomelli, A. New isoxazolidinone and 3,4-dehydro-b-proline derivatives

as antibacterial agents and MAO-inhibitors: A complex balance between two activities. *Eur. J. Med. Chem.* **2016**, *124*, 906-919. doi:10.1016/j.ejmech.2016.09.007

18. Zhang, H.-Z.; Zhao, Z.-L.; Zhou, C.-H. Recent advance in oxazole-based medicinal chemistry. *Eur. J. Med. Chem.* **2018***, 144,* 444–492. doi:10.1016/j.ejmech.2017.12.0

19. Barthel, D.; Schlitzer, M.; Pradel, G. Telithromycin and Quinupristin-Dalfopristin induce delayed death in plasmodium falciparum. *Antimicrob. Agents Chemother*. **2008**, *52,* 774-777. doi:10.1128/aac.00892-07

20. Limoncu, M. E.; Eraç, B.; Gürpinar, T.; Özbilgin, A.; Balcıoğlu, İ. C.; Hoşgör-Limoncu M. Investigation of *in vitro* antileishmanial activity of Moxifloxacin, Linezolid and Caspofungin on *Leishmania tropica* promastigotes. *Turkiye Parazitol Derg.* **2013**, *37*, 1-3. doi:10.5152/tpd.2013.01

21. Córdova-Guerrero, J.; Hernández-Guevara, E.; Ramírez-Zataraín, S.; Núñez-Bautista, M.; Ochoa-Terán, A.; Muñiz-Salazar, R.; Montes-Ávila, J.; López-Angulo, G.; Paniagua-Michel, A.; Nuño Torres, G. A. Antibacterial activity of new oxazolidin-2-one analogues in methicillin-resistant *Staphylococcus aureus* strains. *Int. J. Mol. Sci.* **2014**, *15*, 5277-5291. doi:10.3390/ijms15045277

22. Ochoa-Terán, A.; Rivero, I. Synthesis of enantiopure 1, 3-oxazolidin-2-ones from α-dibenzilamino esters. *ARKIVOC* **2008**, *14*, 330-343.18. doi:http://dx.doi.org/10.3998/ark.5550190.0009.e30

23. Steven, J.; Brickner, S.; Hutchinson, D.; Barbachyn, M.; Mannimen, P.; Ulanowicz, D.; Garmon, S.; Grega, K.; Hendges, S.; Toops, D.; Ford, C.; Zurenko, G. Synthesis and antibacterial activity of U-100592 and U-100766, two oxazolidinone antibacterial agents for the potential treatment of multidrug-resistant gram-positive bacterial infections. *J. Med. Chem.* **1996**, *39*, 673-679.

24. Morán-Ramallal, R.; Liz, R.; and Gotor, V. Regioselective and stereospecific synthesis of enantiopure 1,3-oxazolidin-2-ones by intramolecular ring opening of 2-(Boc-aminomethyl)aziridines. Preparation of the antibiotic Linezolid. *Org. Lett.* **2008**, *10*, 1935-1938. doi:10.1021/ol800443p

25. Tohma, H.; Köksal, E.; Kilic, Ö.; Alan, Y.; Yilmaz, M.; Gülcin, I.; Bursal, E.; Alwasel, S. RP-HPLC/MS/MS Analysis of the phenolic compounds, antioxidant and antimicrobial activities of Salvia L. Species. *Antioxidants* **2016**, *5*, 38. doi:10.3390/antiox5040038

26. Gülçin, I.; Kirecci, E.; Akkemik, E.; Topal, F.; Hisar, O. Turk. Antioxidant, antibacterial, and anticandidal activities of an aquatic plant: duckweed (*Lemna minor L. Lemnaceae*). *J. Biol.* **2010**, *34*, 175-188. doi:10.1016/j.bioorg.2016.12.001

27. Kocyigit, U.; Budak, Y.; Gürdere, M.; Tekin, S.; Köprülü, T.; Ertürk, F.; Özcan, K.; Gülçin, I.; Ceylan, M. Synthesis, characterization, anticancer, antimicrobial and carbonic anhydrase inhibition profiles of novel (3a*R*,4*S*,7*R*,7a*S*)-2-(4-((*E*)-3-(3-aryl)acryloyl) phenyl)-3a,4,7,7a-tetrahydro-1*H*-4,7-methanoisoindole-1,3(2*H*)-dione derivatives. *Bioorg. Chem*. **2017**, *70*,118-125. doi:10.1016/j.bioorg.2016.12.001.

28. Montes-Avila, J.; Díaz-Camacho, S. P.; Willms, K.; De la Cruz-Otero, M. C.; Robert, L. Rivero, I. A.; Delgado-Vargas, F. Bioguided study of the *in vitro* parasitocidal effect on adult *Hymenolepis nana* of the *Psidium sartorianum* (O. Berg Nied.) fruit methanol extract. *Med. Chem. Res.* **2017**, *26*, 2845-2852. doi:10.1007/s00044-017-1983-x

29. Mosmann, T. Rapid colorimetric assay for cellular growth and survival: application to proliferation and cytotoxicity assays. *J. Immunol. Methods* **1983**, *65,* 55-63. doi:10.1016/0022-1759(83)90303-4

30. Hernandez, J.; Goycoolea, F.; Quintero, J.; Acosta, A.; Castañeda, M.; Dominguez, Z.; Robles, R.; Vazquez-Moreno, L.; Velazquez, E.; Astiazaran, H.; Lugo, E.; Velazquez, C. Sonoran propolis: chemical composition and antiproliferative activity on cancer cell lines. *Planta med.* **2007**. *73,* 1469-1474. doi:10.1055/s-2007-990244

31. Desiraju, G. R.; Stainer, T. The weak hydrogen bond in structural chemistry and biology. Oxford Universtiy Press, England. 1999, p. 13.

32. Molecular Operating Environment (MOE), version 2018.01, Chemical Computing Group Inc., Montreal, Quebec, Canada. Available in http://www.chemcomp.com

33. García-Olaiz, G. D.; Alcántar-Zavala, E.; Ochoa-Terán, A.; Cabrera, A.; Muñiz-Salazar, R.; Montes-Ávila, J.; Salazar-Medina, A. J.; Alday-Noriega, E.; Velazquez, C.; Medina-Franco, J. L.; Laniado-Laborín, R. Design, synthesis and evaluation of the antibacterial activity of new Linezolid dipeptide-type analogues. *Bioorg. Chem.* **2020**, *95*, 103483. doi:10.1016/j.bioorg.2019.103483

34. Schuwirth, B. S.; Borovinskaya, M. A.; Hau, C. W.; Zhang, W.; Vila-Sanjurjo, A.; Holton, J. M. Crystal structure of the bacterial ribosome from *Escherichia coli* at 3.5 A resolution. *Science* **2005**, *310*, 827-834. doi:10.1126/science.1117230

35. Shaw, K. J.; Poppe, S.; Schaadt, R.; Brown-Driver, V.; Finn, J.; Pillar, C. M.; Shinabarger, D.; Zurenko, G. In Vitro activity of TR-700, the antibacterial moiety of the produg TR-701, against Linezolid-resistant strains. *Antimicrob. Agents. Chemother*. **2008**, *52*, 4442-4447. doi:10.1128/AAC.00859-08

36. Baily, G.; Garcia, H. H. Chapter 57, Other cestode infections: intestinal cestodes, cysticercosis, other larval cestode infections. In: Manson's Tropical Infectious Diseases, 2014, 23 Ed, London UK: W. B. Saunders; p. 820-832.

37. Lipinski, C. A.; Lombardo, F.; Dominy, B. W.; Feeney, P. J. Experimental and computational approaches to estimate solubility and permeability in drug discovery and development settings. *Adv. Drug Deliv. Rev.* **2001**, *46*, 3-26. doi:10.1016/S0169-409X(00)00129-0.

38. Lipinski, C. A. Lead- and drug-like compounds: the rule-of-five revolution. *Drug Discovery Today: Technologies* **2004**, *1*, 337-341. doi:10.1016/j.ddtec.2004.11.007

Declaration of interests

☒ The authors declare that they have no known competing financial interests or personal relationships that could have appeared to influence the work reported in this paper.

☐The authors declare the following financial interests/personal relationships which may be considered as potential competing interests:

Highlights

- Stereoselective synthesis and characterization of six new Linezolid type compounds.
- The first Linezolid type compounds reported with *in vitro* antiparasitic activity against *Hymenolepis nana.*
- Promising potential as antiparasitic agents because they are more active and induce anatomic damages not observed with Praziquantel.
- These newly Linezolid analogues preserve the cellular integrity and metabolic viability of ARPE-19 cells indicating no *in vitro* cytotoxic affects.